

## Structural, elastic, optical and thermodynamic properties of CdGeP<sub>2</sub> from theoretical prediction

S. R. Zhang<sup>a,\*</sup>, Z. J. Zhu<sup>a</sup>, H. J. Hou<sup>b</sup>, L. H. Xie<sup>c</sup>

<sup>a</sup>*Department of Physics and Information Engineering, Huaihua University, Huaihua 418008, China*

<sup>b</sup>*School of Materials Engineering, Yancheng Institute of Technology, Yancheng 224051, China*

<sup>c</sup>*School of Physics and Electronic Engineering, Sichuan Normal University, Chengdu 610066, China*

We have studied the structural, elastic anisotropy, electronic properties and optical properties of CdGeP<sub>2</sub> crystal by using first-principles method. The effect of pressure on the elastic constants of CdGeP<sub>2</sub> was explored. The changes in the anisotropy of the CdGeP<sub>2</sub> at different pressures were analyzed in detail by three-dimensional (3D) and 2D projections of bulk modulus and Young's modulus. The electronic properties, including the band structure, density of states, were investigated, and it turned out that CdGeP<sub>2</sub> is a semiconductor. Furthermore, we analyze the dielectric function, refractive index, extinction coefficient, absorption coefficient, and electrical conductivity of CdGeP<sub>2</sub> in detail. Finally, the influence laws of temperature and pressure on Debye temperature, heat capacity and Grüneisen parameter are obtained, respectively.

(Received September 14, 2022; Accepted December 2, 2022)

*Keywords:* CdGeP<sub>2</sub>, elastic, Optical properties, Thermodynamic properties

### 1. Introduction

Cadmium germanium phosphorus (CdGeP<sub>2</sub>) crystal is a typical II-IV-V<sub>2</sub> ternary chalcopyrite structure compound semiconductor [1]. Due to its excellent performance in optical parametric oscillator devices and frequency converters, it has attracted widespread attention. Experimentally, Choi et al used the horizontal Bridgeman method to grow CdGeP<sub>2</sub> crystals and study their optical and vibrational properties [2]. Medvedkin et al. studied the photoluminescence properties of CdGeP<sub>2</sub> crystals and the optical properties of epitaxially grown films of CdGeP<sub>2</sub> on GaAs substrates, etc [3]. In theory, Gautam et al have the the structural, electronic and optical properties of CdGeP<sub>2</sub> by linearized augmented plane wave (LAPW) method as implemented in the WIEN2K [4]. Hou et al have calculated the structural, dynamical and thermodynamic properties of CdXP<sub>2</sub> (X = Si, Ge) from first principles [5]. Recently, Rugut et al have calculated the structural stability, surface and photocatalytic properties of CdGeP<sub>2</sub> using the first principle technique [6]. However, at present, most researchers only make various researches on CdGeP<sub>2</sub> crystal as a dilute magnetic material, but ignore the various properties of CdGeP<sub>2</sub> crystal itself. Therefore, in this paper, the first-principles method is used to study and analyze the elastic anisotropy, electronic structures of CdGeP<sub>2</sub> crystals, as well as optical properties such as dielectric constant, refractive index, absorption coefficient, etc.

---

\* Corresponding author: [zefer1979@163.com](mailto:zefer1979@163.com)  
<https://doi.org/10.15251/JOR.2022.186.781>

## 2. Calculation method

All calculations in this article are implemented through CASTEP code[7]. The plane wave basis set is used to expand the electronic wave function, and the Perdew-Burke-Ernzerhof (PBE) exchange correlation energy of the ultrasoft pseudopotential plane wave method and the generalized gradient approximation GGA (Generalized Gradient Approximation) is selected [8, 9]. Through a series of convergence tests, the  $k$  point of the Brillouin zone was selected as the  $7 \times 7 \times 7$  Monkhorst-Pack grid, and the cutoff energy was set to 600.0 eV. The self-consistent field converges to an accuracy of  $1 \times 10^{-6}$  eV. When the difference between the atomic energies calculated for two consecutive times is less than  $1 \times 10^{-7}$  eV, the interaction force between atoms does not exceed 0.03eV/nm, the convergence standard of crystal stress is 0.05GPa, the convergence standard of the maximum displacement of atoms is 0.001nm, Select the valence electron configuration of the atom: Cd:  $4d^{10}5s^2$ , Ge:  $3d^{10}4s^24p^2$ , P:  $3s^23p^3$ . When the above convergence criteria are met, it can be considered that the crystal has reached a structurally stable state, and then the energy band structure, density of states, optical properties are calculated on the basis of the optimized unit cell model.

## 3. Results and discussion

### 3.1. Structural optimization

$\text{CdGeP}_2$  belongs to chalcopyrite structure compound semiconductor, and its crystal structure space group is I-42d (122). The coordinates of the atoms are as follows:

Cd: (0, 0, 0), (0, 1/2, 1/4)

Ge: (0, 0, 1/2), (0, 1/2, 3/4)

P: ( $u$ , 1/4, 1/8), ( $-u$ , 3/4, 1/8), (3/4,  $u$ , 7/8), (1/4,  $-u$ , 7/8). Its unit cell is shown in Fig. 1.

The geometric optimization of the structure is carried out according to the parameters set above. When the system satisfies the set convergence conditions, the system energy reaches the lowest level, and the optimization ends, that is, a stable atomic structure is obtained. The lattice constants  $a$  and  $c$  of the geometrically optimized  $\text{CdGeP}_2$  crystals are listed in Table 1, respectively. According to the analysis in Table 1, the calculated lattice constants  $a$  and  $c$  have little difference with the experimental values [2, 12, 13]. At the same time, it is not difficult to see from the table that the present values of lattice constants ( $a$  and  $c$ ) are in good agreement with available experimental and theoretical values[10, 11], which proves the correctness of the calculation. Subsequent calculations are performed on this optimized structure.

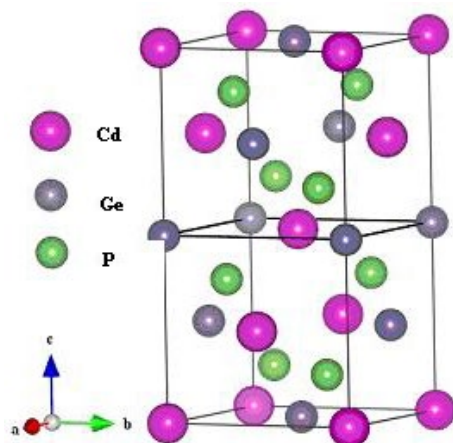


Fig. 1. Crystal structure of CdGeP<sub>2</sub>.

Table 1. Computed lattice constants  $a$  (nm),  $c$  (nm) of CdGeP<sub>2</sub> compared to available experimental and theoretical values.

Present	Theor.		Expt.			
$a$	0.5799	0.5741 <sup>[10]</sup>	0.5811 <sup>[11]</sup>	0.574 <sup>[12]</sup>	0.5741 <sup>[2]</sup>	0.5736 <sup>[13]</sup>
$c$	1.0928	1.077 <sup>[10]</sup>	1.0976 <sup>[11]</sup>	1.0776 <sup>[12]</sup>	1.0775 <sup>[2]</sup>	1.076 <sup>[13]</sup>

### 3.2. Mechanical stability

Tetragonal system CdGeP<sub>2</sub> has six independent elastic constants  $C_{ij}$  ( $C_{11}$ ,  $C_{12}$ ,  $C_{13}$ ,  $C_{33}$ ,  $C_{44}$  and  $C_{66}$ ). The present calculated elastic constants  $C_{ij}$  of CdGeP<sub>2</sub> are listed in Table 2. As we know, the mechanical stability of materials can be judged by the Born stability criterion[14]. According to the calculated elastic constants in Table 2, they satisfy the stability condition, indicating that CdGeP<sub>2</sub> is mechanically stable under 0-20 GPa. According to the calculated elastic constants, we use the Voigt-Ruess-Hill approximations[15-17] to obtain  $B$ ,  $G$ ,  $E$ . Table 3 gives  $B$ ,  $G$ ,  $E$ . By comparing the results in Table 2 and 3, we can see that our calculation results are in good agreement with other theoretical methods[4, 5], indicating the reliability of our calculation.

Table 2. The elastic constants  $C_{ij}$  (GPa) of CdGeP<sub>2</sub> was calculated.

Pressure (GPa)		$C_{11}$	$C_{12}$	$C_{13}$	$C_{33}$	$C_{44}$	$C_{66}$
0	Present	101.2	44.5	49.0	90.0	50.3	47.2
	Ref.[4]	107	61	63.5	102	47	48
	Ref.[5]	102.1	46.7	50.2	89.3	66	69.1
5		127.4	69.8	75.5	110.4	53.4	51.4
10		148.9	90.1	96.3	126.4	53.5	53.8
15		169.9	111.2	117.8	139.5	55.4	54.3
20		190.6	130.5	138.2	150.6	53.3	50.6

Table 3. The elastic modulus ( $B$ ,  $G$  and  $E$ ) (GPa), elastic anisotropic factors ( $A_1$ ,  $A_2$ ,  $A_3$ ,  $A^U$ ,  $A_B$ ,  $A_G$ ) of  $CdGeP_2$ .

Pressure(GPa)	$B$	$G$	$E$	$A_1$	$A_2$	$A_3$	$A^U$	$A_B(\%)$	$A_G(\%)$
0	64.1	37.3	93.7	2.159	2.159	3.330	0.639	0.0598	5.988
0 Theor.[4]	76.73	34.43	89.84						
0 Theor. [5]	65.2	44.47							
5	89.5	38.1	101.0	2.461	2.461	3.569	0.937	0.168	8.541
10	109.7	37.9	101.9	2.588	2.588	3.660	1.104	0.228	9.907
15	129.6	36.9	101.0	3.003	3.003	3.700	1.563	0.540	13.432
20	147.8	33.8	94.4	3.290	3.290	3.368	2.156	1.116	17.578

As is known, the anisotropic elasticity of materials can have a significant impact on material microstructural applications. In order to study the anisotropy of  $CdGeP_2$  in detail, in this work, we study the elastic anisotropy index ( $A^U$ ,  $A_B$ ,  $A_G$ ) and shear anisotropy factor of different crystal planes ( $A_1$ ,  $A_2$  and  $A_3$ ), which can be given by [18-20]:

$$A^U = 5G_V/G_R + B_V/B_R - 6 \quad (1)$$

$$A_B = (B_V - B_R)/(B_V + B_R) \quad (2)$$

$$A_G = (G_V - G_R)/(G_V + G_R) \quad (3)$$

$$A_1 = A_2 = 4C_{44}/(C_{11} + C_{33} - 2C_{13}) \quad (4)$$

$$A_3 = 4C_{66}/(C_{11} + C_{22} - 2C_{12}), C_{66} = (C_{11} - C_{12})/2 \quad (5)$$

The calculated  $A^U$ ,  $A_B$ ,  $A_G$ ,  $A_1$ ,  $A_2$  and  $A_3$  of  $CdGeP_2$  are given in Table 3. For a tetragonal solid,  $A_1 = A_2$  due to the symmetry principle in the tetragonal. The deviation of  $A_1$ ,  $A_2$  and  $A_3$  from 1 increase with increasing pressure, indicating an increase in anisotropy. If  $A^U = A_B = A_G = 0$ , the material is isotropic. The elastic anisotropy indexes in Table 3 are not equal to 0, indicating that  $CdGeP_2$  has a strong degree of anisotropy. The calculated  $A^U$ ,  $A_B$  and  $A_G$  increase with the increase of pressure, indicating that the anisotropy will gradually increase.

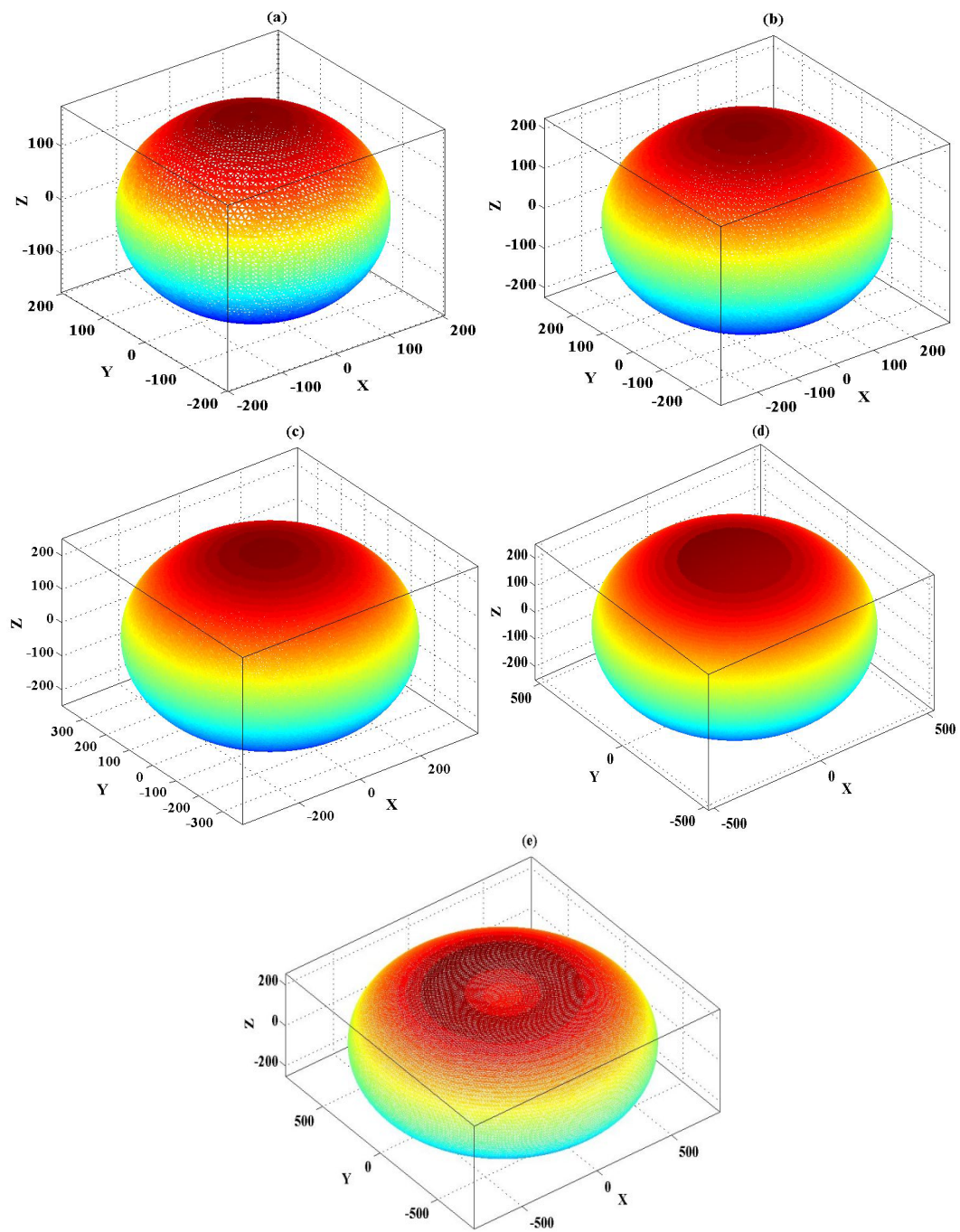


Fig. 2. Representation of direction-dependent Bulk modulus  $B$  (GPa) of  $\text{CdGeP}_2$  ((a): 0 GPa, (b): 5 GPa, (c): 10 GPa, (d): 15 GPa, (e): 20 GPa).

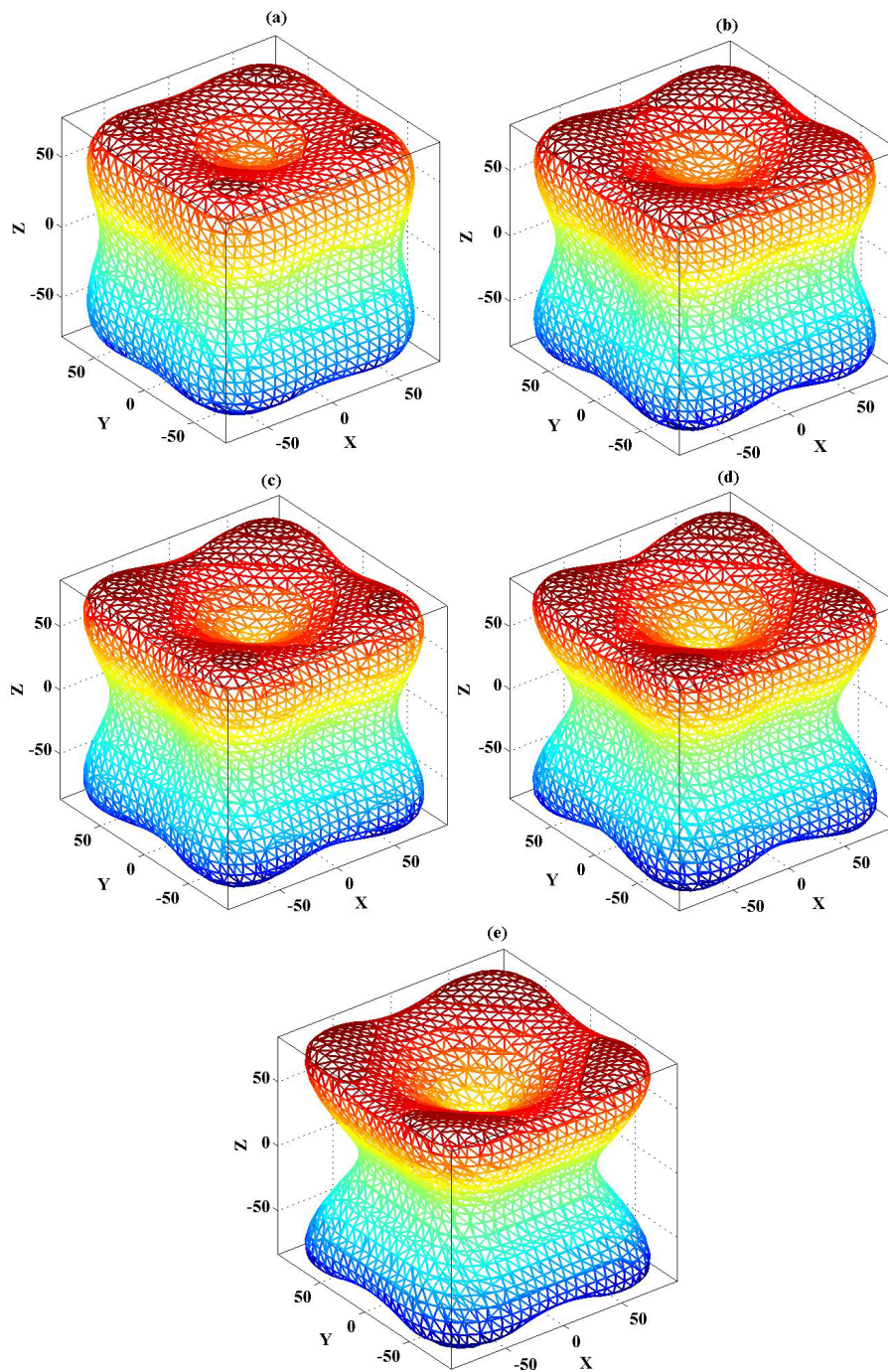


Fig. 3. Representation of direction-dependent of Young's modulus  $E$  (GPa) of  $\text{CdGeP}_2$ . ((a): 0 GPa, (b): 5 GPa, (c): 10 GPa, (d): 15 GPa, (e): 20 GPa).

In addition, 3D construction and 2D projection of bulk modulus and Young's modulus can be used to describe the anisotropy of materials in detail [21]. The 3D surface constructions of  $B$  are plotted in Fig. 2. It can be seen from Fig. 2 that the 3D surface structures at different pressures all deviate from spherical, indicating that the bulk modulus of  $\text{CdGeP}_2$  at different pressures is anisotropic. This is agree with the  $A_B \neq 0$  in Table 3. Likewise, Fig. 3 presents the 3D surface structure of Young's modulus at different pressures. As can be seen in Fig. 3, the 3D plots at different pressures deviate significantly from the sphere, which also indicates that the Young's

modulus of CdGeP<sub>2</sub> is anisotropic.  $A^U \neq 0$  in Table 3 also verifies the anisotropy of Young's modulus. The magnitude of the anisotropy of  $B$  and  $E$  of CdGeP<sub>2</sub> cannot be directly obtained from their 3D surface structure, here we can further obtain it by 2D planar projections.

Table 4. The variations of the Young's modulus  $E$  (GPa) and Bulk modulus  $B$ (GPa) of CdGeP<sub>2</sub> under various pressures.

Pressure (GPa)	$E_{\min}$	$E_{\max}$	$B_{\min}$	$B_{\max}$
0	57.04	117.6	174.2	202.7
5	52.6	132.2	224.5	297.1
10	48.8	138.4	251.3	387.4
15	40.7	144.7	251.2	529.2
20	31.6	140.7	227.3	819.3

Fig. 4-5 shows the 2D planar projections of  $B$  and  $E$  on the  $xy$ ,  $xz$ , and  $yz$  planes. It is obvious that the 2D planar projection on the  $xy$  plane is circular, indicating that  $B$ ,  $E$  of CdGeP<sub>2</sub> are isotropic on the  $xy$  plane. However, the 2D planar projections of  $B$  and  $E$  of CdGeP<sub>2</sub> on the  $xz$  and  $yz$  planes deviate significantly from circularity, which indicates that the  $B$  and  $E$  of CdGeP<sub>2</sub> are anisotropic in the  $xz$  and  $yz$  planes. Table 4 presents the variations of the  $E$  and  $B$  of CdGeP<sub>2</sub> under various pressures. Meanwhile, the magnitude of the elastic anisotropy of CdGeP<sub>2</sub> can be explained in detail by the values of  $B_{\max}/B_{\min}$  and  $E_{\max}/E_{\min}$ . CdGeP<sub>2</sub>, the  $B_{\max}/B_{\min}$  values are 1.1634, 1.3238, 1.5415, 2.1065 and 3.6048 at pressures of 0, 5, 10, 15 and 20 GPa, respectively;  $E_{\max}/E_{\min}$  values are 2.061, 2.514, 2.836, 3.559 and 4.445 at pressures of 0, 5, 10, 15 and 20 GPa, respectively. Therefore, the anisotropy of  $B$  and  $E$  of CdGeP<sub>2</sub> increases with increasing pressure, which is in good agreement with the results obtained for  $A_B$  and  $A^U$ . As results, one can conclude that CdGeP<sub>2</sub> present a strong elastic anisotropy.

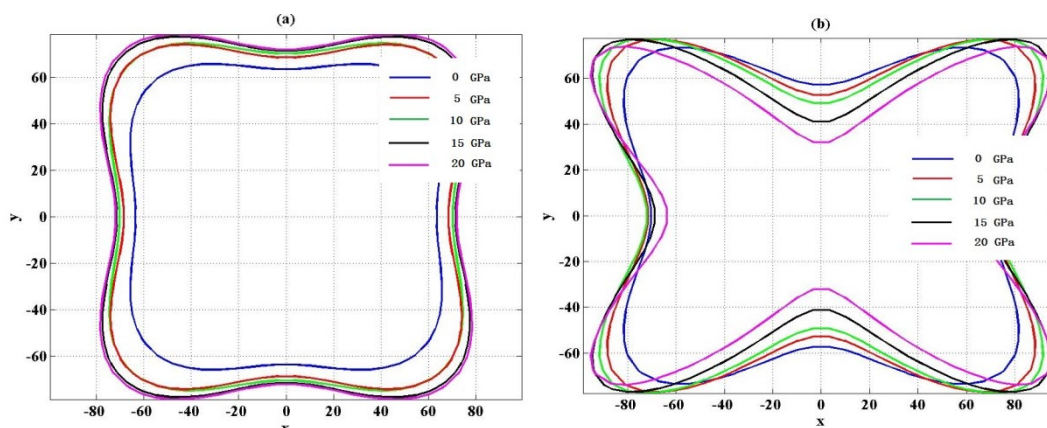


Fig. 4. Planar projections of Young's modulus  $E$  (GPa) of CdGeP<sub>2</sub>.((a): XY plane; (b):XZ and YZ plane).

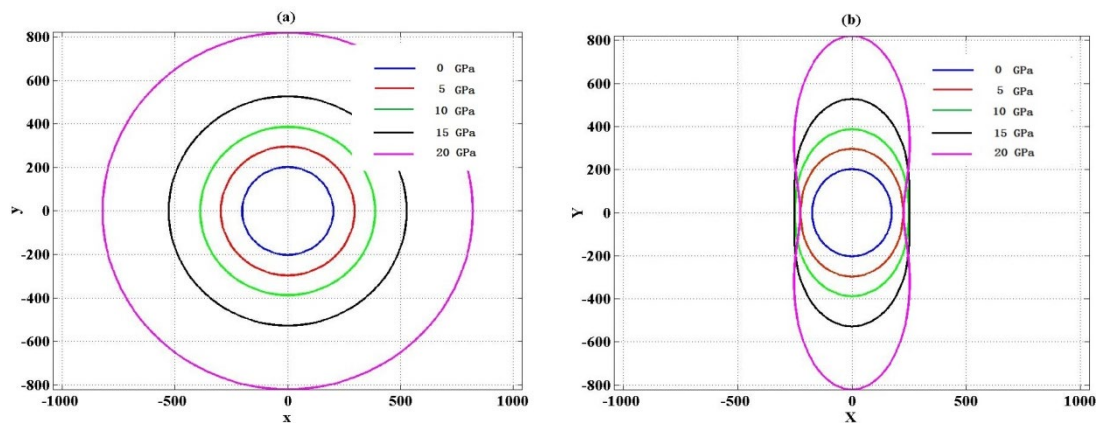


Fig. 5. Planar projections of Bulk modulus  $B$  (GPa) of  $\text{CdGeP}_2$ . ((a):  $XY$  plane; (b):  $XZ$  and  $YZ$  plane).

### 3.2. Electronic structures

Fig. 6 shows the calculated band structure of  $\text{CdGeP}_2$ . From Fig. 6, it can be concluded that the minimum value of the conduction band and the maximum value of the valence band are at the same point  $\Gamma$ , indicating that the  $\text{CdGeP}_2$  crystal is a direct band gap semiconductor. The calculated band gap of  $\text{CdGeP}_2$  crystal is 0.775 eV, which is smaller than the experimental value of 1.72 eV [22]. This is because the GGA functional used in the calculation does not take into account the excited state of the system when solving the Kohn-Sham equation, so that the energy level of the conduction band is relatively low, so the calculated energy band gap is relatively small, but this does not affect to the relative value of the calculated results, it will not affect the theoretical analysis of the electronic structures.

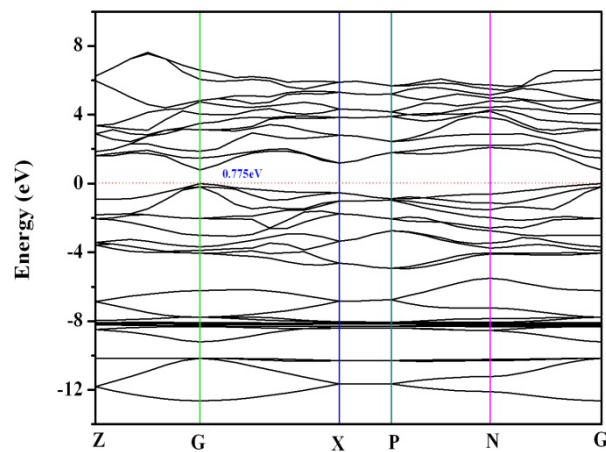


Fig. 6. Band structure of  $\text{CdGeP}_2$  crystal.

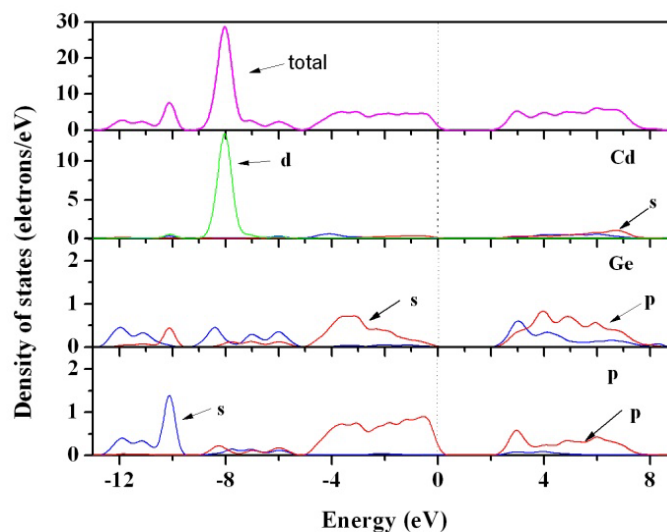


Fig. 7. Total and partial density of states of CdGeP<sub>2</sub> crystal.

Fig. 7 is a density of state of a CdGeP<sub>2</sub> crystal. It can be analyzed from Fig. 7 that the valence band of CdGeP<sub>2</sub> can be divided into three sub-bands, namely the lower valence band in the range of -12.71 eV to -9.48 eV, and the middle valence band in the range of -9.16 eV to -5.36 eV, and the upper valence band in the range of -4.87 eV to 0 eV. In the lower valence band, there is a density of states distribution peak at -10.11 eV, the contribution of which is mainly derived from the 3s orbital of the P atom, hybridized with the 4p orbital of the Ge atom, the 4d and 5s orbital of the Cd atom, and has a strong electron localization. There are also two shoulder peaks, mainly due to the joint action of the 4s orbital of Ge atom and the 3s orbital of P atom. In the mid-valence band, there is a sharp peak of density of states at -8.04 eV, the contribution mainly comes from the 4d orbital of Cd atoms, showing strong electron locality. In the upper valence band, there is a peak of density of states distribution, and the contribution mainly comes from the 3p orbital of P atom and the 4p orbital of Ge atom. The conduction band of CdGeP<sub>2</sub> is composed of a mixture of 3p orbitals of P atoms, 4s and 4p orbitals of Ge atoms, and 5s orbitals of Cd atoms. The top part of the valence band of CdGeP<sub>2</sub> is mainly composed of the 3p orbital electrons of the P atom, while the bottom part of the conduction band is mainly formed by the 3p orbital electrons of the P atom and the 4s orbital electrons of the Ge atom.

### 3.3. Optical properties

In order to correct the problem that the calculated band gap is lower than the experimental value, a scissors correction is introduced in the analysis of optical properties. For CdGeP<sub>2</sub> crystal, the scissors value is selected as 0.945 eV.

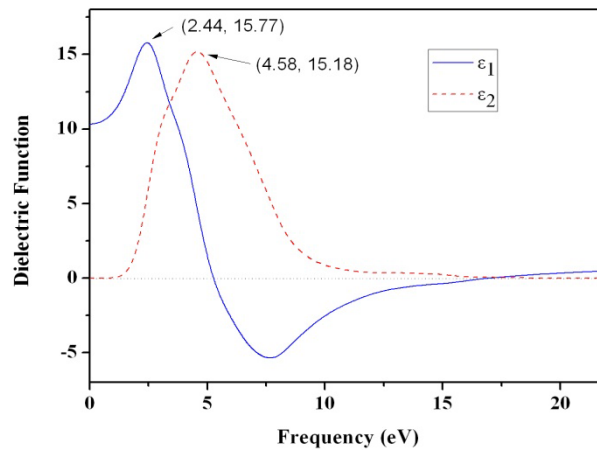


Fig. 8. The real part  $\epsilon_1(\omega)$  and imaginary part  $\epsilon_2(\omega)$  of the dielectric function.

Fig. 8 is a graph showing the relationship between the real part  $\epsilon_1$  and the imaginary part  $\epsilon_2$  of the calculated dielectric function of the CdGeP<sub>2</sub> crystal as a function of the photon energy. It can be seen from the analysis in the figure that in the photon energy range of 0-25 eV, the imaginary part  $\epsilon_2$  has only one maximum value, the maximum value is 15.18, and the corresponding photon energy is 4.58 eV. When the photon energy < 4.58 eV,  $\epsilon_2$  increases gradually; when the photon energy > 4.58 eV,  $\epsilon_2$  decreases sharply. In the whole energy range,  $\epsilon_1$  has a maximum value (real part peak), that is, the maximum value is 15.77 when the photon energy is 2.44 eV; there is a minimum value of -5.37, and the corresponding photon energy is 7.67 eV. In the range of 0-2.44 eV and 7.67-25 eV,  $\epsilon_1$  increases with the increase of photon energy, while in the range of 2.44-7.67 eV,  $\epsilon_1$  decreases sharply with the increase of photon energy. When the energy of the photon is in the range of 5.27-17.07 eV,  $\epsilon_1 < 0$ , it can be seen from the relationship that when the real numbers  $\omega$  and  $\epsilon_1$  are both less than zero, the wave vector  $\kappa$  is an imaginary number, then in this energy range, light cannot pass through the CdGeP<sub>2</sub> crystal.

Fig. 9 shows the relationship between the real part (Re) and the imaginary part (Im) of the calculated optical conductivity of the CdGeP<sub>2</sub> crystal with the photon energy. At 0-1.62 eV, the real part (Re) of the optical conductivity is almost zero, because the band gap of the CdGeP<sub>2</sub> crystal is 1.72 eV, so the photon energy is less than this band gap, and the transition of electrons is forbidden. When the photon energy is 5.02 eV, the real part (Re) of the optical conductivity reaches a maximum of 8.77 fs<sup>-1</sup>.

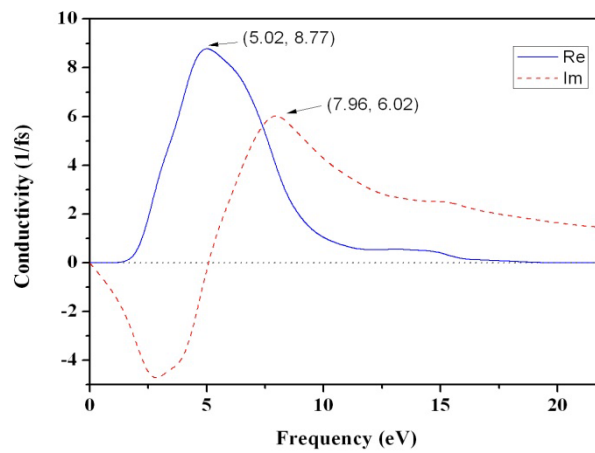


Fig. 9. Optical conductivity of CdGeP<sub>2</sub>.

Fig. 10 is the calculated reflectivity of the CdGeP<sub>2</sub> crystal. It can be seen from the figure that when the photon energy is in the range of 0-25 eV, there are two main peaks on the reflection spectrum of CdGeP<sub>2</sub> crystal, that is, when the photon energy is 11 eV, the peak is 0.76; when the photon energy is 16.08 eV, with a peak value of 0.73. The maximum reflectivity of CdGeP<sub>2</sub> crystal is 76%. When the photon energy is in the range of 0-11 eV and 14.43-16.08 eV, the reflectivity increases gradually with the increase of the photon energy; when the photon energy is in the range of 11-14.43 eV and 16.08-22 eV, the reflectivity increases with the photon energy increase and decrease sharply.

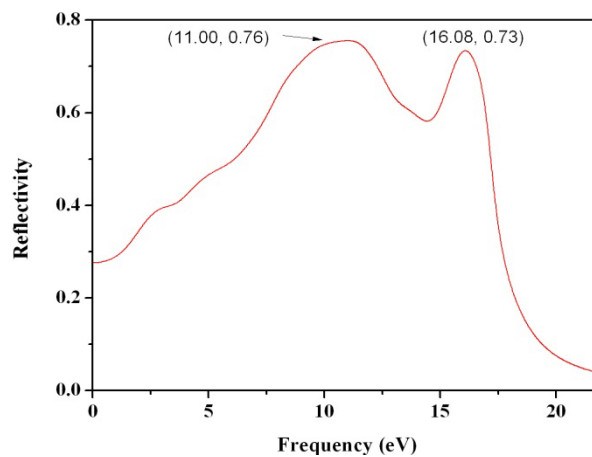


Fig. 10. The Reflectivity spectrum of CdGeP<sub>2</sub> crystal.

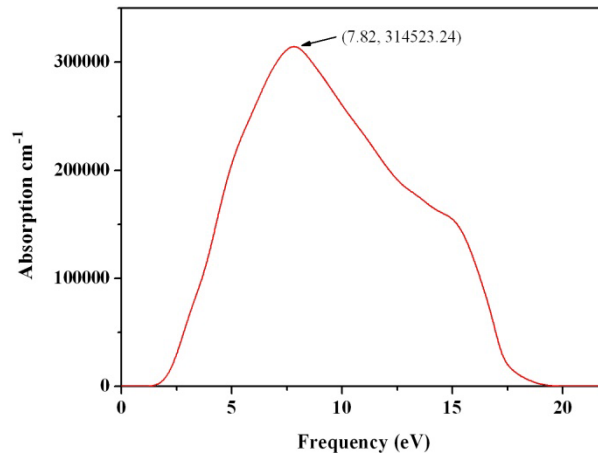


Fig. 11. The Absorption coefficients of CdGeP<sub>2</sub> crystal.

Fig. 11 is a graph showing the relationship between the calculated absorption coefficient of CdGeP<sub>2</sub> crystal and photon energy. In the range of photon energy  $< 1.33$  eV and photon energy  $> 19.63$  eV, the absorption coefficient of this crystal is close to zero. When the energy  $> 1.33$  eV, the absorption coefficient starts to increase until it reaches a maximum value of  $314523.24 \text{ cm}^{-1}$  at  $7.82$  eV, after which the absorption coefficient starts to decrease as the energy of the photon increases, and finally tends to zero.

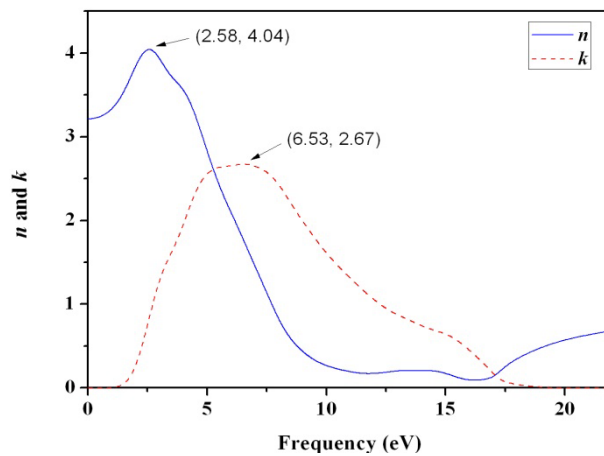


Fig. 12. The refractive index  $n$  and the extinction coefficient  $k$  of CdGeP<sub>2</sub> crystal.

The refractive index  $n$  and extinction coefficient  $k$  of CdGeP<sub>2</sub> crystals are calculated from  $n^2 - k^2 = \epsilon_1$  and  $2nk = \epsilon_2$  are shown in Fig. 12. From the analysis of the figure, it can be seen that the static refractive index  $n_0$  of the CdGeP<sub>2</sub> crystal is 3.21, the maximum refractive index is 4.04, and the corresponding photon energy is 2.58 eV. In the energy range of 0-2.58 eV, the refractive index  $n$  increases gradually; in the energy range of 2.58-11.76 eV, the refractive index  $n$  decreases sharply, almost zero; in the energy range of 11.76-25 eV, the refractive index  $n$  gradually increases.

The region where the peak value of the extinction coefficient  $k$  of the CdGeP<sub>2</sub> crystal is located corresponds to the minimum value region of  $\varepsilon_1$  in Fig. 8. The extinction coefficient  $k$  and the imaginary part  $\varepsilon_2$  of the dielectric function have similar trends, reaching a maximum value of 2.67 when the photon energy is 6.53 eV, while the corresponding  $\varepsilon_2$  reaches a maximum value of 15.18 when the photon energy is 4.58 eV, indicating the change of the extinction coefficient lag the change in  $\varepsilon_2$ . When the photon energy is in the range of 5.27 -17.07 eV,  $k > n$ , from  $n^2 - k^2 = \varepsilon_1$ ,  $\varepsilon_1 < 0$ . It can be concluded that in this range, light cannot propagate in the CdGeP<sub>2</sub> crystal.

### 3.4. Thermodynamic properties

To study the thermodynamic properties of crystals, the quasi-harmonic Debye model developed by Blanco et al [23]. First, the CASTEP code was used to calculate the total energy versus volume of CdGeP<sub>2</sub> crystals near the equilibrium structure, as shown in Fig 13. The calculated curves were fitted with the Birch-Murnaghan equation of state [24]. The equilibrium structure volume of CdGeP<sub>2</sub> crystal were obtained by fitting. The lattice constants  $a$  and  $c$  of the CdGeP<sub>2</sub> crystal obtained from the fitting are 0.5809 nm and 1.0946 nm, respectively. The fitted lattice constants  $a$  and  $c$  agree well with the optimized and experimental or other theoretical values in Table 1.

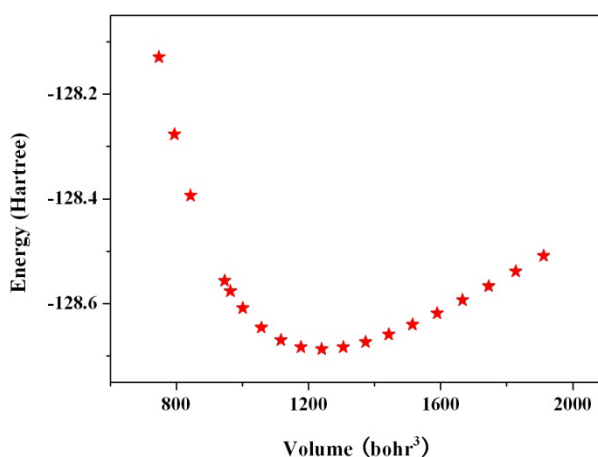


Fig. 13. Total energy vs. volume of CdGeP<sub>2</sub> crystal.

Fig.14 shows the relationship between Debye temperature and temperature of CdGeP<sub>2</sub> crystal under different pressures. According to Fig. 14, it can be obtained that the Debye temperature gradually decreases with the increase of temperature when the pressure is 0, 5, 10, 15 and 20 GPa, respectively. It can be concluded that the higher the pressure, the smaller the effect of temperature. At zero pressure, it is possible to fit the Debye temperature and the relationship with temperature  $T = 372.46 - 0.02687T$ . The calculated Debye temperature of CdGeP<sub>2</sub> crystal at  $T = 0$ ,  $P = 0$  pressure = 370.44 K, which is in good agreement with other theoretical calculation results = 342.01 K [25], indicating that the calculation is correct.

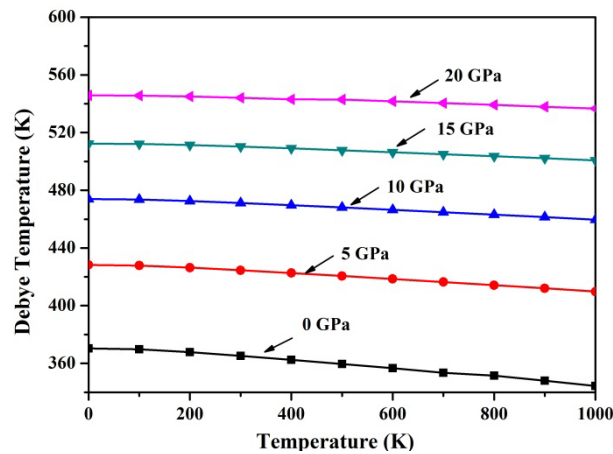


Fig. 14. Debye temperature  $\Theta$  of the  $\text{CdGeP}_2$  at various pressures and temperatures.

The Grüneisen parameter  $\gamma$  is an important parameter. Table 5 lists the Grüneisen parameter  $\gamma$  values at different temperatures and pressures. The analysis shows that under a given pressure, the  $\gamma$  value increases with the increase of temperature. However, at a given temperature, the value of  $\gamma$  decreases with increasing pressure. At 300 K ( $P = 0$ ), the  $\gamma$  value was 2.357.

Table 5. The values of Grüneisen parameter  $\gamma$  at different temperatures and pressures.

$T$ (K)	$P$ (GPa)				
	0	5	10	15	20
0	2.329	2.071	1.911	1.795	1.704
200	2.343	2.078	1.915	1.798	1.706
400	2.372	2.093	1.924	1.804	1.711
600	2.404	2.109	1.935	1.812	1.715
800	2.434	2.127	1.946	1.820	1.721
1000	2.476	2.145	1.958	1.828	1.728

Fig. 15 shows the relationship between the heat capacity and temperature of  $\text{CdGeP}_2$  crystals under different pressures. It can be seen from Fig. 15 that under different pressures,  $C_V$  is affected by temperature at low temperature, and increases sharply with the increase of temperature, and is proportional to  $T^3$ . When the temperature increases to a certain extent,  $C_V$  increases with temperature. The rise was almost close to the Dulong-Petit limit value (Fig. 15). However, the constant pressure heat capacity  $C_P$  increases sharply with the increase of temperature and is proportional to  $T^3$ , and will continue to increase in a linear manner at high temperature  $T > 400$  K.

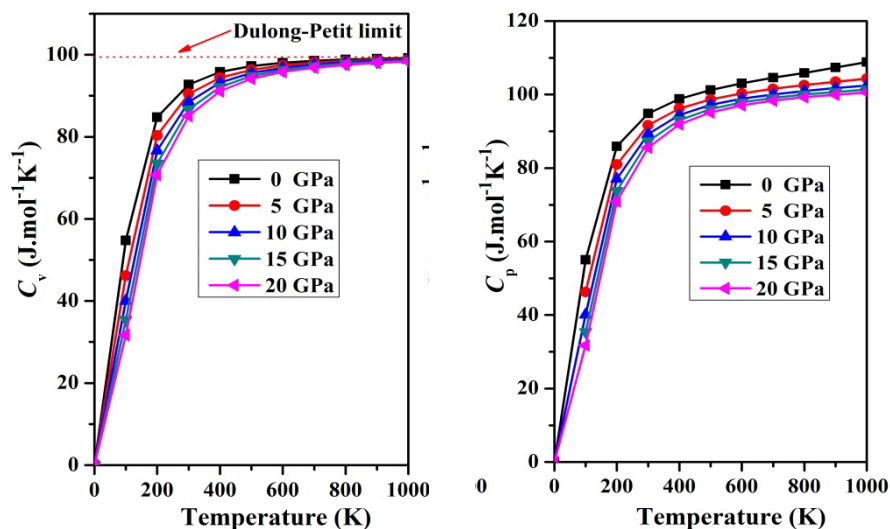


Fig. 15. Heat capacity  $C_V$  and  $C_p$  of the  $\text{CdGeP}_2$  at various pressures and temperatures

#### 4. Conclusions

In this paper, first-principles calculations were used to study the elastic anisotropy, electronic structures and optical properties of  $\text{CdGeP}_2$ . The anisotropy of  $E$  and  $B$  of  $\text{CdGeP}_2$  increases continuously with increasing pressure. The calculation results show that the  $\text{CdGeP}_2$  crystal is a direct bandgap semiconductor. The dielectric function, refractive index, extinction coefficient, reflection coefficient, absorption coefficient and optical conductivity of  $\text{CdGeP}_2$  was studied and analyzed. In the range of 0-20GPa and 0-1000K, the Debye temperature of  $\text{CdGeP}_2$  crystal, as well as the Grüneisen parameters and heat capacity changes with temperature or pressure were calculated.

#### Acknowledgments

This work is supported by the Key Laboratory of agricultural ecological prevention and control of Huaihua.

#### References

- [1] Gennadiy A. Medvedkin, Valeriy G. Voevodin, J. Opt. Soc. Am. B 22, 1884 (2005); <https://doi.org/10.1364/JOSAB.22.001884>
- [2] I. H. Choi, D. H. Lee, Y. D. Choi, Y. M. Yu and P. Y. Yu, J. Korean Phys. Soc. 44, 403 (2004).
- [3] G. A. Medvedkin, V. M. Smirnov, T. Ishibashi and K. Sato, J. Phys. Chem. Sol. 66, 2015 (2005); <https://doi.org/10.1016/j.jpcs.2005.10.164>
- [4] Ruchita Gautam, Pravesh Singh, Sheetal Sharma, Sarita Kumari and A. S. Verma, Mat. Sci. Semicon. Proc. 40, 727 (2015); <https://doi.org/10.1016/j.mssp.2015.07.005>

- [5] H. J. Hou, H. J. Zhu, S. P. Li, T. J. Li, L. Tian and J. W. Yang, *Indian J Phys.* 92, 315(2018); <https://doi.org/10.1007/s12648-017-1109-9>
- [6] Elkana Rugut, Daniel Joubert and Glenn Jones, *Comp. Mater. Sci.* 187, 110099 (2021); <https://doi.org/10.1016/j.commatsci.2020.110099>
- [7] S. J. Clark, M. D. Segall and C. J. Pickard, *Z. Kristallogr* 220, 567 (2005); <https://doi.org/10.1524/zkri.220.5.567.65075>
- [8] D. Vanderbilt, *Phys. Rev. B* 41, 7892(1990); <https://doi.org/10.1103/PhysRevB.41.7892>
- [9] J. P. Perdew, K. Burke and M. Ernzerhof, *Phys. Rev. Lett.* 77, 3865(1996); <https://doi.org/10.1103/PhysRevLett.77.3865>
- [10] A. A. Vaipolin *Solid State Phys.*, 15, 1430(1973)
- [11] V. L. Shaposhnikov, A. V. Krivosheeva, V. E. Borisenko, J. L. Lazzari and Arnaud F. Avitayad, *Phys. Rev. B* 85, 205201(2012)
- [12] O. Madelung, U. Rössler and M. Schulz *Landolt-Börnstein in Condensed Matter, Ternary Compounds, Organic Semiconductors, New Series, Group III, Vol.41E* (Springer-Verlag, Berlin) (2000); <https://doi.org/10.1007/b72741>
- [13] J. L. Shay, J. H. Wernick *Ternary Chalcopyrite Semiconductors* (Pergamon Press, Great Britain, ), p. 8.(1975)
- [14] M. Born, K. Huang *Dynamical Theory of Crystal Lattices* (Oxford: Clarendon) (1954)
- [15] W. Voigt *Lehrbuch der Kristallphysik* Teubner Leipzig (1928)
- [16] A. Reuss, *Z. Angew. Math. Mech.* 9, 49 (1929); <https://doi.org/10.1002/zamm.19290090104>
- [17] R. Hill, *Proc. Phys. Soc.* 65, 349 (1952); <https://doi.org/10.1088/0370-1298/65/5/307>
- [18] S. I. Ranganathan and M. Ostojca-Starzewski, *Phys. Rev. Lett.* 101, 055504 (2008); <https://doi.org/10.1103/PhysRevLett.101.055504>
- [19] F. W. Vahldiek, *S A Mersol Anisotropy in Single Crystal Refractory Compounds Vols. 1 & 2*, Plenum Press (1968); <https://doi.org/10.1007/978-1-4899-5307-0>
- [20] P. Ravindran, L. Fast, P. A. Korzhavyi, B. Johansson, J. Wills and O. Eriksson, *J. Appl. Phys.* 84, 4891(1998); <https://doi.org/10.1063/1.368733>
- [21] J. F. Nye, *Physical Properties of Crystals*, Oxford University Press Oxford (1985)
- [22] J. L. Shay, E. Buehler, J. H. Wernick, *Phys. Rev. B* 4, 2479 (1971); <https://doi.org/10.1103/PhysRevB.4.2479>
- [23] M. A. Blanco, E. Francisco and V. Luana, *Comput. Phys. Commun.* 158, 57 (2004); <https://doi.org/10.1016/j.comphy.2003.12.001>
- [24] F. Birch, *Phys. Rev.* 71, 809 (1947); <https://doi.org/10.1103/PhysRev.71.809>
- [25] V. Kumar, A. K. Shrivastava, R. Banerji and D. Dhirhe, *Solid State Commun.* 149, 1008 (2009); <https://doi.org/10.1016/j.ssc.2009.04.003>